

## Beyond simulated versus observed: gaining insight to shallow ground water – surface water exchange using visualization and sensitivity analysis.

Gilbert Barth<sup>1</sup>, Karen MacClune<sup>1</sup>, Nabil Shafike<sup>2</sup>, Deborah L. Hathaway<sup>1</sup>

<sup>1</sup>S.S.P. & A., [gbarth@sspa.com](mailto:gbarth@sspa.com), [karen@sspa.com](mailto:karen@sspa.com), [dhathaway@sspa.com](mailto:dhathaway@sspa.com), Boulder, CO, USA

<sup>2</sup>New Mexico Office of the State Engineer, [nabil.shafike@state.nm.us](mailto:nabil.shafike@state.nm.us), Albuquerque, NM, USA

### ABSTRACT

A riparian-zone groundwater model, one of a suite of models representing shallow groundwater conditions and exchanges between surface water and shallow groundwater within the floodplain of the Rio Grande, is used to demonstrate the benefits of going beyond the typical comparison of simulated versus observed. Evaluation of a groundwater model often focuses on the comparison of a limited number of observations to their simulated equivalents. Examination of details beyond such comparisons provides considerable insight to the physical system, as approximated by the numerical simulation. Methods demonstrated include (1) three-dimensional flux visualization, to assess the temporal and spatial variability in magnitude and direction of flux between the ground water and the river and drains, (2) sensitivity maps providing insight into the spatial distribution of a parameter's importance, and (3) composite sensitivities to compare importance across different parameter and observation types. Examination of these details will be a critical component of future work that may address questions such as: how much flow is required to sustain desirable riparian habitat, what are the impacts of various mitigation efforts, and which mitigation effort will be most effective?

### INTRODUCTION

The Lower Albuquerque (LAB) Riparian model is one of the Middle Rio Grande Riparian Models [MacClune *et al.*, 2006], all of which were created using MODFLOW-2000 [Harbaugh *et al.*, 2000]. The Riparian Models were developed to study the exchange between the river and shallow groundwater and the potential impact of restoration efforts. The 4-layer LAB model extends from the I-40 crossing of the Rio Grande in Albuquerque, to just below the Bernalillo-Valencia County line and uses 250- by 125-foot grid cells, with the longer cell axis orientated along the general direction of the river. With a total of 312 rows and 194 columns the domain covers about 15 miles of river. The lateral extents of the active domain are delineated by the riverside drains. The result is a relatively long, narrow domain, about 0.5 miles wide (Figure 1).

The conceptual components of the model consist of, (1) the river as a spatially and temporally varying source and sink, (2) the drains functioning primarily as a sink, but having the capability to serve as a source under the right circumstances, and (3) regional aquifer flow serving as a source or sink depending on the observed heads in the area. River stage and geometry were determined using a hydraulic model for the Rio Grande, FLO-2D [Tetra Tech, Inc., 2004]. The MODFLOW simulations presented in this work were of the Spring 2004 pulse consisting of low flow during the preceding winter, followed by the rise and fall of the spring-runoff pulse (Figure 2).

As with many models, a sparse observation set limits the ability to assess the model performance, both in terms of the spatial and temporal variability of residuals. As a result the conceptual model itself is pressed into service, not as formal prior information, but

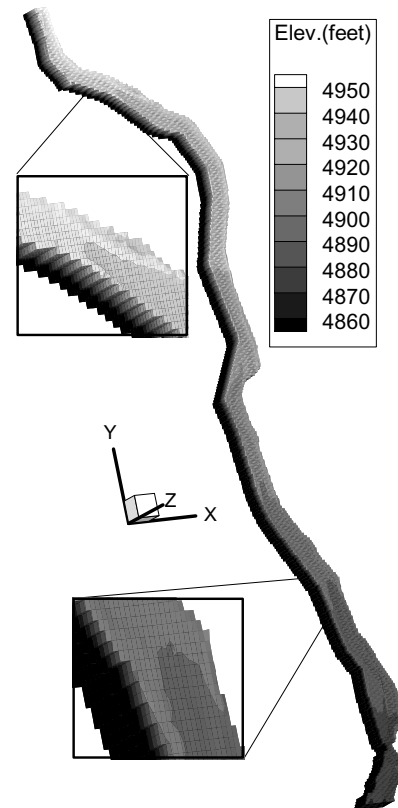
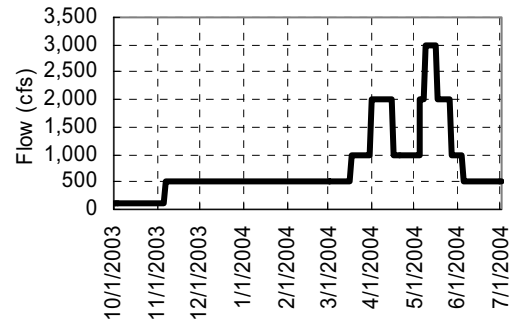


Figure 1. 3D image of the LAB riparian model domain, grid-cell surface elevation.

simply as a qualitative constraint on the simulation results. A well developed set of expectations, based on the conceptual model, are compared to the simulated results, examining both spatial and temporal variability in order to identify inconsistencies between the simulated and conceptualized physical system. Emphasis is placed on the fundamental insight that can be gained from postprocessing and visualization of simulated results.

This paper demonstrates existing, readily available methods being used as part of the ongoing development and application of the Riparian Models. For each of these methods, the emphasis in this work is to garner more insight into the hydrologic system than can be expected from a comparison of simulated versus observed heads. The methods applied to the LAB model and presented here include (1) three-dimensional flux visualization, (2) mapping of sensitivities, and (3) summarizing sensitivities using composite scaled sensitivities (css) [Hill, 1998]. The first two rely heavily on the processing and visualization of large amounts of data, providing qualitative and quantitative insight into the simulated system while the last provides summary values. Three-dimensional flux visualization is self-explanatory. Sensitivity maps display the spatial distribution of a simulated value's change for a change in parameter value, such as the change in head for a specified change in hydraulic conductivity. The css combine individual sensitivities of different observations allowing comparison even when combining observation types and considering multiple parameters.



**Figure 2. Spring 2004 river flow**

## METHODS

### Flux Post Processing and Visualization

A variety of post processing approaches are available ranging from simple pieces of code, output viewers such as the USGS ModelViewer [Hsieh and Winston, 2002], to sophisticated graphical user interfaces. This work uses simple pieces of code to extract the data from the binary output files, and process it for the visualization software, Tecplot®, although any 3D-visualization and animation software would suffice. Code to extract fluxes from the binary output files is available from a variety of sources (e.g. USGS's MODFLOW webpage and the University of Alabama's MT3DMS website). The postprocessing code simply reads and writes the fluxes, providing a formatted file for the visualization software along with some basic labels to help identify different flux types (e.g., GHB, RIV, front-face). For this work the 2004 spring-pulse LAB binary output file is postprocessed and the formatted results plotted with the visualization software. Plots typically focus on individual stress packages such as the river or general-head boundary packages, to assess their interaction with the aquifer.

### Sensitivity Maps

Sensitivity maps were generated for the LAB model for a variety of parameters including the layer-one storage parameter and riparian ET, RIP-ET [Maddock and Baird, 2003]. For this work, 2004 spring-pulse sensitivity maps are generated using either the sensitivity-equation method, using MODFLOW-2000, or the perturbation-based approach, using PESTv10 [Watermark Numerical Computing, 2004], or both. In addition to differences due to the calculation method, the two approaches have advantages and disadvantages in terms of implementation. For example, while the sensitivity-equation method typically provides a more accurate assessment it is limited to parameters for which MODFLOW-2000 has been coded to calculate the sensitivity equations. A perturbation-based method, such as PEST or UCODE [Poeter et al., 2005], can calculate sensitivities for virtually any parameter. A full assessment of the differences between sensitivity-equation and perturbation-based sensitivities is beyond the scope of this brief presentation; the two methods are presented together simply to remind and advocate the use of multiple methods in order to increase the potential for discriminating between results and artifacts.

Generation of sensitivity maps from MODFLOW-2000 is a simple matter of creating additional input files, running the simulation and then plotting the sensitivity data. MODFLOW-2000 provides output of one-

percent scaled sensitivities for every grid cell in the model [Hill *et al.*, 2000, p. 71] and can produce the one-percent scaled, head-sensitivity maps for a wide range of parameters. PEST can save the Jacobian matrix in a binary-file form, which is then postprocessed using the included utilities, and the results plotted as sensitivity maps. Since MODFLOW-2000 generates one-percent scaled sensitivities the sensitivity-map values from the PEST-generated Jacobian matrix will be 100 times larger than the MODFLOW-2000 values, when the parameter has a value equal to 1.0.

Perturbation-based approaches generally provide greater flexibility in terms of the parameters and observations evaluated. For example, in the LAB model the RIP-ET package was used to represent riparian-zone evapotranspiration. Since the RIP-ET package is not part of the official MODFLOW-2000 release MODFLOW-2000 does not include sensitivity equations for RIP-ET and the perturbation-based method was used to create the sensitivity maps.

### Composite Scaled Sensitivities

As opposed to the flux and sensitivity maps, css are typically used to provide a lumped summary by combining individual scaled sensitivities. A css indicates the total amount of information provided by the observations for the estimation of a single parameter [Hill, 1998], or a measure of the parameter importance in determining the simulated values.

## RESULTS

### Flux Post Processing and Visualization

Figure 3a shows the flux from the RIV package to the aquifer, demonstrating spatial and temporal variations. The lightest shading, occurring where there are no river or drain cells, indicates zero flux. The darkest shading indicates flow from the aquifer to the RIV cells, and the dark grey represents flux from the RIV cells to the aquifer.

Post processing the binary outputs, creating a separate TECPLOT zone for each timestep allows the possibility of animating with time. The zones are displayed in succession to create an animated image, which cannot be demonstrated in print, but Figure 3a shows three of the zones representing flux at three different times.

Figure 3b shows the same stress-period 6 data, but uses the flux magnitude as the abscissa ordinate. The lighter shading, protruding upwards, represents positive flux: from the river to aquifer. The darker shading on the portions extending downward represents flux from the aquifer to the river. This simple change in display provides an alternative way to examine the results, the animation of which provides an intuitive visualization of the magnitude and direction of river-aquifer interaction.

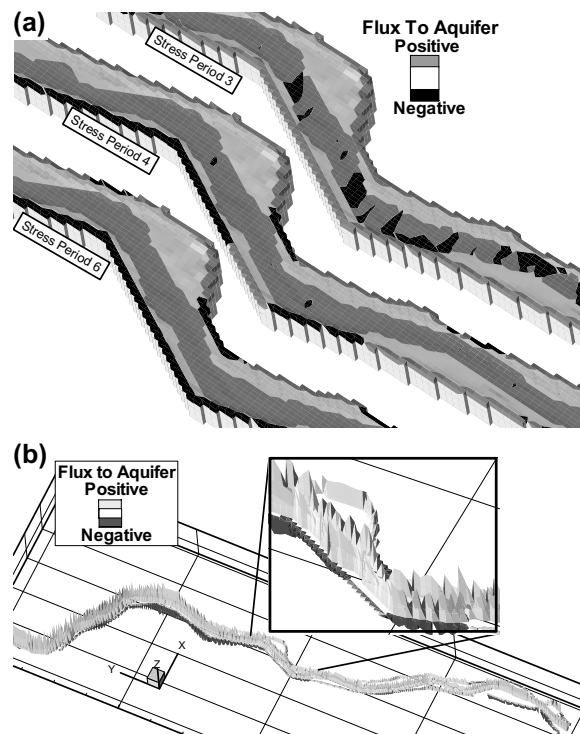


**Figure 3. Time and space varying RIV-to-aquifer fluxes (a) standard X, Y, Z (b) flux magnitude as Z coordinate.**

### Sensitivity Maps

The layer-one-storage-parameter sensitivity maps in Figure 4a and b were calculated using sensitivity-equation and perturbation methods, respectively, and indicate the amount of information that a head observation provides for the layer-one storage parameter, for a subregion of the LAB model. Zero-sensitivity values, in cells where boundary conditions such as the RIV package control heads, are more accurately depicted using the sensitivity-equation method. Differences between the two methods are

relatively minor, especially if relative importance is the primary concern. However, it should be noted that even such small differences may result in significantly different outcomes over the course of a parameter-estimation run.

Figure 5 demonstrates the transient nature of the sensitivity maps for the layer-1 storage parameter (a and b) and class-A vegetation ET (c and d) for a subregion of the LAB model domain. As the river stage rises and aquifer storage fills, the sensitivities are mostly negative indicating that an increase in storage coefficient will decrease the simulated head (Figure 5a), while in Figure 5b the values are mostly positive since the river stage is dropping and an increased storage coefficient results in heads staying higher at the end of the stress period. In addition to the sign, the maps indicate a shift in the high-sensitivity locations. In Figure 5c, the greater magnitude sensitivity locations indicate areas that, for increased class-A vegetation ET rates, result in the least increase

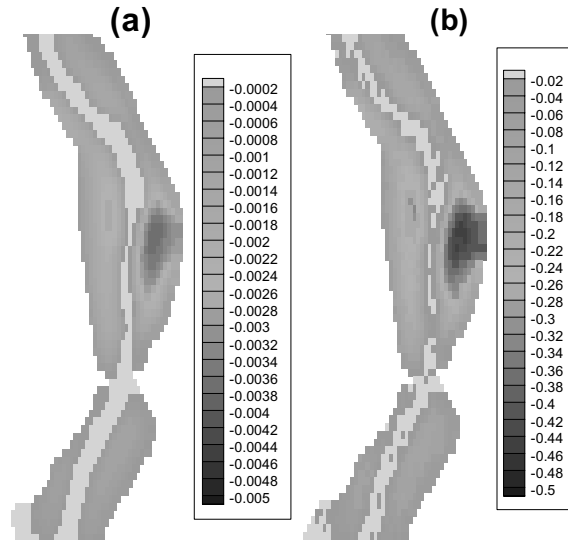


Figure 4. Head-sensitivity maps for storage parameter, (a) MODFLOW-2000 1% scaled sensitivities, and (b) PEST generated sensitivities.

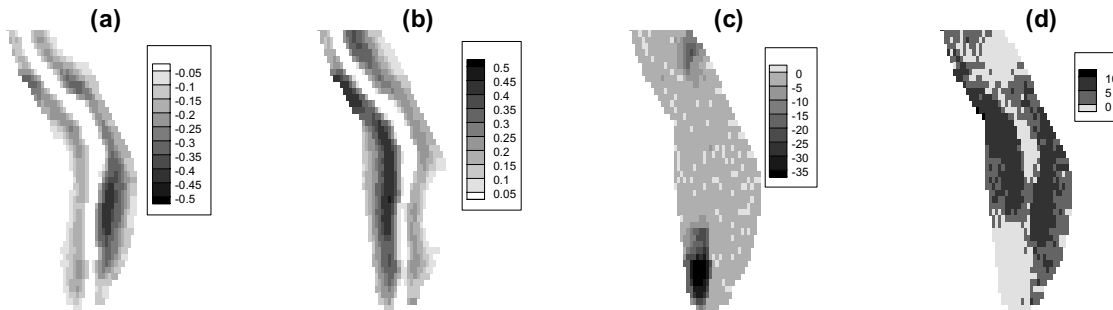


Figure 5. Head sensitivity to (a) layer-1 storage parameter for rising and (b) falling river stage, (c) class-A vegetation ET for rising and (d) falling river stage.

in heads as river stage rises during the stress period. In contrast, Figure 5d shows large areas of positive sensitivity as the river stage falls indicating that, contrary to intuition, a higher ET rate will increase heads in that particular falling-stage stress period, as discussed below.

### Composite Scaled Sensitivities

The selected css (Figure 6) provide perspective on parameter importance using, for simplicity, only the head observations from the entire domain. Other results, not presented, would often include flow observations as well. The ET rate for class-E vegetation has greater overall impact than the rate for the other vegetation classes, A – D. The Rio Grande conductance (*RIO\_C*) has slightly more potential to influence heads than the layer-one storage parameter (*ss1\_lpf*), but considerably less than drain conductance (*DRN\_C*).

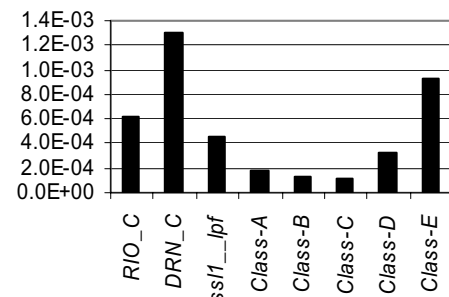


Figure 6. Selected composite scaled sensitivities

### DISCUSSION/CONCLUSIONS

The simulations and results presented here are preliminary. While specific features are discussed for the sake of illustration, the primary objective is to demonstrate and advocate the overall process of viewing fluxes, sensitivities, and interpreting css.

The spatial and temporal variation of flux from the river to the aquifer reflects the proximity of groundwater levels to the ground surface. In Figure 3a, the stress-period 3 low river stage results in spatial variability of flux to and from the aquifer. In stress period 6, with higher river stage, this variability virtually disappears and the aquifer gains along the entire river subreach shown in Figure 3a. At lower flows the drains function primarily as a source of water, which may reflect the model's use of a fixed-in-time drain stage, and is a potential target for future refinement. As river stage rises the drains perform a more typical role, removing water from the aquifer. The same discussion can be applied to Figure 3b; the format simply provides an alternative method of presentation which may better convey differences in flux magnitude and direction.

The sensitivity maps show a strong dependence on river stage: *ss1\_lpf* is more sensitive on the right side of the river (Figure 5a) for rising stage and more sensitive on the left side for falling stage (Figure 5b). These visualizations should lead to questions such as: is this behavior expected, do the drain elevations dominate the system response, and what is the uncertainty of the drain elevations? Similarly, in Figure 5d, does the positive sensitivity of riparian ET with falling river stage simply reflect a combination of head and depth-dependent extinction depth, or is the model somehow misrepresenting the physical system?

The domination of the ET *css* by class *E* should raise basic questions about the simulation centered around determining the reasons that class *E* dominates other species and whether that is consistent with the physical system. For example, (1) is class *E* the spatially dominate species, (2) does class *E* have a greater extinction depth and ET rate, and (3) does class *E* preferentially occupy locations most conducive to ET, such as the lowest elevation locations.

Each of the results discussed should provoke very basic questions, such as “why does the drain function as a conveyance in a particular stress period?”, or “will replacing a riparian vegetation species have much impact on the hydrologic system?”, forcing a more thorough understanding of the numerical representation and in so doing, a check against the conceptual expectation of the physical system.

## REFERENCES

- Hsieh, P.A., and Winston, R.B., 2002, User's Guide to Model Viewer, A Program for Three-Dimensional Visualization of Ground-water Model Results: U.S. Geological Survey Open-File Report 02-106, 18 p.
- Harbaugh, A.W., E.R. Banta, M.C. Hill, and M.G. McDonald, 2000. MODFLOW-2000, the U.S. Geological Survey modular ground-water model—User guide to modularization concepts and the ground-water flow process, Open File Report 00-92, 121 p.
- Hill, M. C., 1998. Methods and guidelines for effective model calibration, USGS WRIR 98-4005, 96 p.
- Hill, M.C., E. R. Banta, A. W. Harbaugh, and E. R. Anderman, 2000. MODFLOW-2000, The U.S. Geological Survey modular ground-water model – User guide to the observation, sensitivity, and parameters-estimation processes and three post processing programs, Open File Report 00-184, 210p.
- MacClune, K. L., G. Barth, N. Shafike, D Hathaway, 2006. High-Resolution Groundwater Models for the Assessment of Riparian Restoration Options and River Conveyance Efficiency, MODFLOW2006 conference proceedings.
- Maddock III, T., and K. J. Baird, 2003. A riparian evapotranspiration package for MODFLOW-2000, HWR No. 02-03, Dept. of Hyd and Water Res., University of Arizona, Tucson, AZ.
- Poeter, E.P., Hill, M.C., Banta, E.R., Mehl, Steffen, and Christensen, Steen, 2005, UCODE\_2005 and Six Other Computer Codes for Universal Sensitivity Analysis, Calibration, and Uncertainty Evaluation: U.S. Geological Survey Techniques and Methods 6-A11, 283p.
- Tetra Tech, Inc. 2004. Development of the Middle Rio Grande FLO-2D flood routing model, Cochiti Dam to Elephant Butte Reservoir, Surface Water Group, Albuquerque, New Mexico. Prepared for the Bosque Initiative Group, U.S. Fish and Wildlife Service and the U.S. Army Corps of Engineers.
- Watermark Numerical Computing, 2004. Model-Independent Parameter Estimation User Manual: 5th Edition, 336 p.